Published in final edited form as:
Exp Neurol. 2009 December ; 220(2): 293–302. doi:10.1016/j.expneurol.2009.08.034.

The Development of Recurrent Seizures after Continuous Intrahippocampal Infusion of Methionine Sulfoximine in Rats:

A Video-Intracranial Electroencephalographic Study

Yue Wang[1], **Hitten P. Zaveri**[2], **Tih-Shih W Lee**[3], and **Tore Eid**[4,*]

[1]Department of Neurosurgery, Yale University School of Medicine, New Haven, CT, USA

[2]Department of Neurology, Yale University School of Medicine, New Haven, CT, USA

[3]Department of Psychiatry, Yale University School of Medicine, New Haven, CT, USA

[4]Department of Laboratory Medicine, Yale University School of Medicine, New Haven, CT, USA

Abstract

Glutamine synthetase is deficient in astrocytes in the epileptogenic hippocampus in human mesial temporal lobe epilepsy (MTLE). To explore the role of this deficiency in the pathophysiology of MTLE, rats were continuously infused with the glutamine synthetase inhibitor methionine sulfoximine (MSO, 0.625 μg/h) or 0.9% NaCl (saline control) unilaterally into the hippocampus. The seizures caused by MSO were assessed by video-intracranial electroencephalogram (EEG) monitoring. All (28 of 28) of the MSO-treated animals and none (0 of 12) of the saline-treated animals developed recurrent seizures. Most recurrent seizures appeared in clusters of 2 days' duration (median; range, 1 to 12 days). The first cluster was characterized by frequent, predominantly Stage I seizures, which presented after the first 9.5 h of infusion (median; range, 5.5 to 31.7 h). Subsequent clusters of less-frequent, mainly partial seizures occurred after a clinically silent interval of 7.1 days (median; range, 1.8 to 16.2 days). The ictal intracranial EEGs shared several characteristics with recordings of partial seizures in humans, such as a distinct evolution of the amplitude and frequency of the EEG signal. The neuropathology caused by MSO had similarities to hippocampal sclerosis in 23.1% of cases, whereas 26.9% of the animals had minimal neuronal loss in the hippocampus. Moderate to severe diffuse neuronal loss was observed in 50% of the animals. In conclusion, the model of intrahippocampal MSO infusion replicates key features of human MTLE and may represent a useful tool for further studies of the cellular, molecular and electrophysiological mechanisms of this disorder.

Keywords

Astrocyte; epilepsy; glutamate; glutamine synthetase; hippocampal sclerosis; intracranial EEG

*Corresponding Author Tore Eid, M.D., Ph.D., Department of Laboratory Medicine, Yale University School of Medicine, 333 Cedar Street, P.O. Box 208035, New Haven, CT 06520-8035, USA, tore.eid@yale.edu, Telephone: +1 203 785 4928, FAX: +1 203 737 2159.

Introduction

Patients with medically intractable mesial temporal lobe epilepsy (MTLE) are deficient in the enzyme glutamine synthetase in specific areas of the epileptogenic mesial temporal lobe such as the hippocampus (Eid, et al., 2004;van der Hel, et al., 2005) and the amygdala (Steffens, et al., 2005). Studies have shown that the protein expression and activity of glutamine synthetase are reduced in subpopulations of astrocytes in areas CA1, CA3 and the dentate gyrus of the hippocampus (Eid, et al., 2004;van der Hel, et al., 2005) and in the amygdala (Steffens, et al., 2005). Because glutamine synthetase is critical for the conversion of neurotransmitter glutamate to glutamine, a deficiency in the enzyme has been postulated to slow the clearance of glutamate from the extracellular space, with high extracellular glutamate concentrations as a possible consequence (Eid, et al., 2004).

Remarkably high concentrations of extracellular glutamate, measured by in vivo microdialysis, are indeed present in the epileptogenic vs. the nonepileptogenic hippocampus during the interictal period in patients with MTLE (Cavus, et al., 2005). Furthermore, extracellular hippocampal glutamate increases sixfold above the interictal level during a seizure and remains elevated for an extended period in the epileptogenic vs. the nonepileptogenic hippocampus after cessation of the seizure activity (During and Spencer, 1993). Isotope (13C) tracer studies performed during epilepsy surgery indicate that the accumulation and impaired clearance of glutamate in MTLE are due to a slowing in the conversion of hippocampal glutamate to glutamine (Petroff, et al., 2002). Based on these observations, we have hypothesized that the deficiency in glutamine synthetase is a possible causative factor for the perturbed glutamate homeostasis in MTLE (Eid, et al., 2004). Moreover, because glutamate is a potent excitotoxin, we have hypothesized further that the deficiency in glutamine synthetase leads to recurrent seizures and neuropathological features typical of MTLE (Eid, et al., 2004).

In order to explore the biological effects of the glutamine synthetase deficiency in the mesial temporal lobe in epilepsy, we recently developed an animal model of chronic glutamine synthetase deficiency in the hippocampus (Eid, et al., 2008). To this end we employed a continuous infusion of the glutamine synthetase inhibitor methionine sulfoximine (MSO) unilaterally into the hippocampus in freely moving rats. This treatment led to sustained inhibition of glutamine synthetase in the infused hippocampus, with normal enzyme activity in the contralateral hemisphere. The rationale for the sustained inhibition of glutamine synthetase was to replicate the situation in human MTLE (where glutamine synthetase is consistently deficient in the sclerotic hippocampus) as closely as possible. The animals developed recurrent seizures and neuropathological changes that in some cases were similar to hippocampal sclerosis, which is one of the hallmarks of human MTLE (Gloor, 1991;Sommer, 1880). We have now extended these studies to involve a comprehensive, long-term evaluation of the seizures caused by intrahippocampal MSO infusion. Using continuous video-intracranial electroencephalogram (EEG) monitoring, we have quantified and characterized, in more detail than previously (Eid, et al., 2008), several aspects of the seizures in the MSO-treated animals. We report for the first time how the seizures caused by MSO-infusion progress from an initial period of multiple, predominantly subclinical and Stage I seizures, via a clinically silent interval, to clusters of recurrent seizures. Our hypothesis is that the present model can be used to study the cellular, molecular and electrophysiological mechanisms of seizure generation caused by intrahippocampal MSO administration. We postulate further that the model replicates key features of human MTLE and therefore is a valuable tool for discovery of novel biomarkers and therapeutics of this disease.

Materials and methods

Chemicals and animals

All chemicals were obtained from Sigma Chemical Co. (St. Louis, Mo.) unless otherwise noted. Male Sprague Dawley rats were used in this study (200 to 250 g; Charles River Laboratories, Wilmington, Mass.). The rats had free access to food and water and were housed on a 12-h light/dark cycle, with lights on from 7 a.m. to 7 p.m. The animal care and use procedures were approved by the Institutional Animal Care and Use Committee of Yale University. All experiments were performed in accordance with current guidelines.

Surgery

The rats were anesthetized with 1 to 2% Isoflurane (Baxter, Deerfield, Ill.) in O_2 and placed in a stereotaxic frame (David Kopf Instruments, Tujunga, Calif.). A 30-gauge stainless steel cannula attached to a plastic pedestal (Plastics One, Roanoke, Va.) was introduced through a burr hole in the skull and into the right hippocampus, using the following coordinates with bregma as the reference: AP = −5.6 mm, ML = 5.3 mm, DV = −6.5 mm. The cannula was cemented to the skull using cyanoacrylate and connected via plastic tubing to a subcutaneously implanted Alzet osmotic pump (Model 2004, Durect Corp., Cupertino, Calif.). This pump holds a total volume of 200 μL and delivers a continuous flow of 0.25 μL/h for ~28 days (as per manufacturer's specifications). One set of pumps was filled with MSO (2.5 mg/mL; dissolved in 0.9% NaCl) to achieve a delivery of 0.625 μg of MSO per h. Another set of pumps was filled with 0.9% NaCl (saline) and implanted in control animals.

In one set of animals (17 MSO-treated and 9 saline-treated), two unipolar electrodes (E363/2/SPC stainless steel electrode, Plastics One) with bare diameter of 0.200 mm and insulated diameter of 0.230 mm, were introduced into the dorsal hippocampus to record continuous intrahippocampal EEG activity in freely moving, awake animals. Approximately 1 mm of insulation was stripped from the tip of each electrode. The coordinates used were as follows: AP = −3.3 mm, ML = 2.5 mm, DV = −3.9 mm. One electrode was inserted into each hippocampus. A third depth electrode was positioned in the white matter of the cerebellum (AP = −10.3 mm, ML = 3.0 mm, DV = −6.5 mm) to serve as the reference. A screw electrode was positioned in the occipital bone to serve as the ground.

A common problem with continuous, long-term EEG recordings of freely moving rats is electrode failure, which eventually occurs due to partial or complete detachment of the electrodes from the animal's skull. The risk of electrode detachment can be minimized by using epidural screw electrodes, which adhere more securely to the skull, rather than intracranial depths. Moreover, intermittent rather than continuous EEG monitoring provides less mechanical stress on the electrodes from the external cables. Although screw electrodes do not provide recordings from the hippocampus, they allow documentation of seizures when the seizures spread to involve the neocortex. In order to monitor animals for extended time periods, 11 additional MSO-treated and 3 saline-treated animals were subjected to intermittent EEG recordings using epidural screw electrodes. Four stainless steel epidural screw electrodes (Plastics One) were implanted to record cortical EEG activity. Two electrodes (one in each hemisphere) were positioned in the epidural space overlying the parietal neocortex. A third electrode was positioned in the epidural space near lambda to serve as the reference. A fourth electrode was positioned over the occipital bone (not touching the dura) to serve as the ground.

The female socket contacts on the end of each electrode were inserted into a plastic pedestal (Plastics One), and the entire implantation was secured by UV light cured acrylated urethane adhesive (Loctite 3106 Light Cure Adhesive, Henkel Corp., Rocky Hill, Conn.).

Video-intracranial EEG monitoring, seizure quantitation and statistics

The experimental setup for recording video-EEG was adapted from Bertram et al. (Bertram, et al., 1997). The rats were placed individually in custom-made Plexiglas cages. A spring-covered, 6-channel cable was connected to the electrode pedestal on one end and to a commutator (Plastics One) on the other. A second cable connected the commutator to the digital EEG recording unit (Ceegraph Vision LTM, Natus Bio-logic Systems Corp., Mundelein, Ill.). Digital cameras with infrared light detection capacity were used to record animal behavior (two cages per camera). The digital video signal was encoded and synchronized to the digital EEG signals. Seizures were identified by visual inspection of the EEG record. As detailed in Avoli and Gloor (1994) seizures were defined by EEG characteristics and not by the duration of the discharge. Specifically, seizures displayed distinct signal changes from background (interictal) activity. Such signal changes included sustained rhythmic or spiking EEG patters and a clear evolution of signal characteristics from onset to termination. Subclinical seizures were distinguished from clinical seizures by examination of the video record. The start and stop points of seizures were identified by the following commonly used method. By visual inspection of the EEG, we determined a point that was unequivocally within the seizure. Next we moved backward in time to determine the seizure start time as the first point where the EEG was different from background activity and forward in time to establish the seizure end time. The video record was examined to stage the seizures, using a modification of Racine's criteria (Racine, et al., 1973), as follows: Subclinical, no remarkable behavior; Stage I, immobilization, eye blinking, twitching of vibrissae and mouth movements; Stage II, head nodding, often accompanied by facial clonus; Stage III, forelimb clonus; Stage IV, rearing; Stage V, rearing, falling and generalized convulsions. Recurrent seizures were defined as ≥2 seizures of Stage III or higher at least 1 h apart.

The temporal distribution and total number of seizures in the depth electrode and screw electrode-implanted animals were determined by reviewing the entire EEG record. To characterize the duration and frequency of seizures at different Racine stages during the initial cluster (which was defined as ≥2 seizures with complete recovery between each seizure and with both seizures occurring within a 24-h period), an average of 20 seizures from each of the depth electrode-implanted animals were randomly chosen from this period and staged by examining the corresponding video record. The duration of each seizure was noted as well. Seizures during later clusters were classified and characterized separately, but because the number of seizures during these clusters was typically <20, all the seizures during each of the later clusters were staged. Kruskal-Wallis Analysis of Variance on Ranks, followed by Dunn's test, was used to compare the frequencies and durations of different seizure stages. Mann-Whitney Rank Sum test was used to compare each seizure stage between the initial and later clusters. A p value of <0.05 was determined as a statistically significant difference.

Histology and nomenclature

Rats were anesthetized with Isoflurane and perfused transcardially with saline followed by 4% paraformaldehyde in phosphate buffer (PB; 0.1M, pH 7.4). The brains were removed and left in the same fixative overnight at 4°C and then transferred to 20% sucrose (dissolved in PB) the next day. After 48 h at 4°C, the brains were removed from the sucrose solution and quickly frozen with isopentane chilled to approximately −70°C in a slush of dry ice and ethanol. The brains were stored at −80°C until being sectioned on a sliding microtome at 80-μm thickness. Every fifth section was mounted on gelatin-coated slides and stained with cresyl violet. The slides were covered and examined under a light microscope. The subdivisions of the hippocampus are in accordance with the work of Lorente de Nó (Lorente de Nó, 1934) with the modifications suggested by Amaral and Insausti (Amaral and Insausti, 1990). In brief, the hippocampus is divided into (a) the subiculum, (b) the Ammon's horn (hippocampus proper),

which comprises fields CA1-3, and (c) the dentate gyrus, which includes the molecular layer, granule cell layer and polymorphic layer of the hilus.

Results

We first established the proportion of rats that developed recurrent seizures. Seventeen MSO-infused and 9 saline-infused rats were monitored by continuous video and hippocampal depth electrode EEG recordings for a maximum of 27 days (median, 18 days; range, 14 to 27 days; Fig. 1). An additional 11 MSO-infused and 3 saline-infused rats were monitored by intermittent video and epidural screw electrode recordings for a maximum of 82 days. All (28 of 28; Fig. 1) of the MSO-treated animals and none (0 of 12) of the saline-treated animals developed recurrent seizures. None of the MSO-treated or saline-treated animals died unexpectedly after they had recovered from surgery.

We then assessed the temporal distribution of the seizures by first examining the depth electrode-implanted animals, which had been continuously monitored since the implantation of the MSO delivery pump. Sixteen (94%) of these animals exhibited an initial cluster of recurrent seizures that began within the first 48 h after the initiation of MSO infusion (Fig. 1). The median interval from the start of surgery until the first seizure commenced was 9.5 h (range, 5.5 to 31.7 h). The highest median frequency of seizures during the initial cluster was observed during postsurgery days (PSDs) 1 (7 seizures per 24 h; range, 0 to 196) and 2 (19 seizures per 24 h; range, 4 to 114; Fig. 2). Then at PSD 3 the seizure frequency began to decline markedly, from a median of 5 seizures per 24 h (range, 0 to 41) to a median of 0 seizures per 24 h (range, 0 to 7) at PSD 4. The seizure frequency during PSD 2 was significantly higher than the seizure frequencies during PSDs 4 to 7 ($p < 0.001$, n = 17, Kruskal-Wallis analysis followed by Dunn's test, Fig. 2).

After the initial cluster of recurrent seizures, 9 of 16 animals (56%) experienced a seizure-free period of >24 h, followed by another cluster of recurrent seizures. The median duration of the period from the initial to the second cluster was 7.1 days (range, 1.8 to 16.2 days; Fig. 1). However, this measure is probably an underestimate, as the relatively short (9 to 27 days) recordings of the depth electrode-implanted group may have missed the presence of later clusters of recurrent seizures in some animals. This notion is supported by the observation that 10 (91%) of the 11 epidural screw electrode-implanted animals (which were generally recorded for longer periods) exhibited later clusters of seizures. It was noticed that two of the MSO-treated rats (#041607 and #041907; Fig. 1) exhibited a prolonged initial cluster of seizures, lasting 7 to 12 days, with fewer than 10 seizures per 24 h during this time. Subsequent histological examination revealed that the MSO infusion cannula was inserted into the extreme dorsal portion of the hippocampus in these animals, whereas all the other rats, which displayed a shorter initial cluster of seizures, had the infusion cannula placed in the ventral hippocampus, which was the intended target. One MSO-treated animal (#032607; Fig. 1) did not experience any seizures immediately after MSO infusion but did experience clusters of seizures at PSDs 11 and 12 and 15 to 18. We could not find an explanation for the lack of initial seizures in this animal.

There was a striking tendency for the seizures to occur in clusters, which were defined as ≥2 seizures with complete recovery between each seizure and with both seizures occurring within a 24-h period (Fig. 1). For example, in the depth electrode-implanted animals, the median number of seizures in the second cluster was 11 (range, 6 to 20; number of clusters counted, 6) and in the third cluster was 14 (range, 10 to 33; number of clusters counted, 3). The seizure frequency during the initial cluster was significantly higher than during later clusters (Fig.1, $p < 0.01$, Mann-Whitney Rank Sum test). Multiple clusters of seizures were seen in several

animals, particularly in the epidural screw electrode-implanted group, which exhibited clusters of recurrent seizures as late as 45 days postsurgery.

Staging of the seizures was then performed. As many as 228 (75%) of the 305 seizures staged during the initial cluster were classified as either subclinical or Stage I seizures (Fig. 3A). The frequency of Stage I seizures during this period was >10 times greater than the frequency of any other seizure type ($p < 0.001$, Kruskal-Wallis analysis followed by Dunn's test; Fig. 3A). However, no differences among the seizure stages were found during later clusters ($p > 0.05$, Kruskal-Wallis analysis followed by Dunn's test; Fig. 3B). We then assessed the duration of seizures at different stages. Stage III seizures lasted approximately 20 seconds longer during the initial cluster compared to later clusters ($p < 0.01$, Mann-Whitney Rank Sum test, Fig. 4A). Also, the subclinical seizures were significantly shorter than the seizures at other stages during later clusters, whereas no such difference was seen during the initial cluster ($p < 0.001$, Kruskal-Wallis analysis followed by Dunn's test; Fig. 4B).

Visual inspection of the EEG record unambiguously revealed that the seizure activity was morphologically distinct from background (interictal) activity. The ictal EEGs shared several classic characteristics with the EEGs of partial seizures in humans, such as low voltage fast activity, high amplitude rhythmic activity, sharp waves, spikes, polyspikes and a distinct evolution of the amplitude and frequency of the EEG signal. Some of the morphological characteristics of these ictal EEGs are depicted in Fig. 5. Two types of seizures were observed. The first, termed Type I Seizures (Fig. 5A and B), contained a single uninterrupted phase of seizure activity. A second type of ictal event, termed Type II Seizures (Fig. 5C) was different from Type I seizures in that it consisted of two distinct phases of paroxysmal discharges separated by a phase of quiet EEG.

Both Type I and II Seizures could be initiated by high-frequency EEG activity, followed by a decrease in signal frequency and gradual increase in amplitude. These changes were accompanied by more regular EEG activity. The high-amplitude, low-frequency, regular EEG discharges typically lasted 30 to 60 seconds, though Type I Seizures of longer duration were sometimes observed. In Type II Seizures this phase of EEG activity was followed by quiet EEG, which indicated the beginning of the second phase of the seizure. The quiet period usually lasted 10 to 30 seconds before a 5- to 20-second period of high-amplitude spike discharges appeared in the Type II Seizure. At times, following the end of the seizure we observed very low-amplitude rhythmic delta activity, which continued for several seconds. A longer-duration Type I Seizure, which began with distinct high-frequency activity, is displayed in Fig. 5B. This seizure is followed by very well-defined delta activity. The seizure types (Types I and II) did not appear to correlate to specific behavioral seizure patterns (subclinical or Stage I–V seizures).

Finally, we evaluated the hippocampal pathology of the MSO-treated and saline-treated animals (Fig. 1 and 6). Four types of histological changes were observed in the MSO-treated group ($n = 26$), as follows: Grade I (26.9%, 7 of 26 animals), minimal neuronal loss (diameter, <100 μm) and gliosis around the infusion cannula track, no patterned involvement of other hippocampal subfields; Grade II (42.3%, 11 of 26 animals), moderate neuronal loss (diameter, >100μm) around the infusion cannula track, no necrosis present; Grade III (7.7%, 2 of 26 animals), moderate to extensive neuronal loss (diameter, >100 μm) with accompanying necrosis, involving and usually extending beyond the hippocampus; Grade IV (23.1%, 6 of 26 animals), sclerosis-like changes of the hippocampus with gross atrophy and loss of neurons in CA1 to CA3 and the dentate hilus. All of the saline-treated animals (12 of 12) showed Grade I histological changes.

Discussion

Many patients with MTLE cannot control their seizures with current antiepileptic drugs; furthermore, the seizures in MTLE occur intermittently and without warning. Discovery of novel approaches aimed at treating and predicting the impending seizures in MTLE is therefore important. However, the discovery of such approaches has been lagging, partly due to the fact that the cellular, molecular and electrophysiological mechanisms of seizure generation in MTLE are poorly understood. Part of the reason for the lack of such knowledge is that few animal models efficiently, reliably and accurately replicate key features of human MTLE. For example, the models of systemic kainic acid (Ben-Ari, 1985) and pilocarpine injections (Turski, et al., 1983) are characterized by severe, often lethal, convulsive status epilepticus initially, followed by widespread brain damage that in many cases is not representative of human MTLE. The models of amygdala kindling (McIntyre, et al., 1999) and hyperthermic seizures (Dube, et al., 2000) generally do not result in spontaneous recurrent seizures, and models that lead to spontaneous recurrent seizures such as tetanus toxin injection (Jefferys and Walker, 2006) often do so unreliably.

Continuous infusion of MSO unilaterally into the hippocampus in rats, as described here, consistently results in episodes of recurrent, mainly partial seizures. The prevalence of the recurrent seizures is 100%, and the mortality rate is minimal. Moreover, the neuropathological sequelae of MSO infusion are mild to modest, with many animals showing minimal neuronal loss in the hippocampus by Nissl staining. Notably, a subpopulation of animals exhibits neuropathological changes that are reminiscent of hippocampal sclerosis, which is one of the hallmarks of MTLE (Gloor, 1991;Sommer, 1880). Finally, patients with MTLE are deficient in glutamine synthetase in the epileptogenic hippocampus (Eid, et al., 2004;van der Hel, et al., 2005), and infusion of MSO into the rat hippocampus consistently replicates this feature (Eid, et al., 2008). Thus, the present model may prove to be a highly useful tool for studies of the mechanism of seizure generation—ictogenesis—in MTLE.

It is important to note that the present model is different from earlier rodent studies using systemic administration of MSO (Folbergrova, et al., 1969;Szegedy, 1978). In these studies, certain strains of mice and rats developed severe, generalized convulsions after an intraperitoneal injection of MSO (Bernard-Helary, et al., 2000;Subbalakshmi and Murthy, 1981). The convulsions lasted for 24 to 48 h and were often associated with considerable mortality. No episodes of later, recurrent seizures were reported in the systemically MSO-treated animals that survived the initial event.

The present model is characterized by an initial cluster of predominantly partial seizures, a period of clinical silence and, eventually, episodes of seizures that may recur for several weeks. Even though MSO is administered as a continuous infusion over approximately 28 days, the pattern of seizures during the initial cluster is different from that of the later episodes. Firstly, there is a higher frequency of seizures during the initial vs. later clusters. Secondly, the majority of seizures during the initial cluster are Stage I, whereas no such predominance is seen during later episodes. It is not clear why these differences are present, but factors related to the surgical procedure, such as tissue inflammation (Vezzani and Granata, 2005) and perturbations in stress hormones (Joels, 2009), may be involved. It is also possible that the initial seizures trigger a sequence of events that modulate the type and frequency of subsequent seizures (Ben-Ari, 2008), although the concept that seizures beget seizures is somewhat controversial (Blume, 2006).

Regardless of the cause, the seizures in the present model appear to progress from an initial event of numerous, rather homogeneous seizures, via a clinically silent period, to more sporadic episodes of less-frequent, more-heterogeneous seizures. This sequence of events, although

contracted in time, is reminiscent of human MTLE. Many patients with this disease have experienced an “initial precipitating injury,” such as prolonged febrile seizures, several years prior to the onset of recurrent seizures (Cendes, et al., 1993;French, et al., 1993). It has been postulated that the initial precipitating injury triggers a sequence of events that, during a clinically silent “latent period,” “ripens” into an epileptogenic focus. It has been postulated further that appropriate therapeutic interventions initiated during the latent period may halt epileptogenesis and completely prevent the development of epilepsy. Thus, it is possible that the present model can be used to study the evolution of epilepsy—epileptogenesis—and the effects of therapeutic interventions during the latent period.

There is a striking tendency for the seizures in the present model to occur in clusters that are separated by longer, seizure-free intervals. Clustering of seizures has been reported in other animal models of temporal lobe epilepsy (Dudek, et al., 2006;Goffin, et al., 2007) and in human partial epilepsies (Balish, et al., 1991;Bauer and Burr, 2001). Perhaps one of the most common types of seizure clustering is seen in catamenial epilepsy (Penovich and Helmers, 2008). In this disorder, which affects almost 40% of women with epilepsy, there is an increased frequency of seizures during a certain period of the menstrual cycle (Herzog, et al., 2004). Mechanisms such as: (a) alterations in brain water concentrations, (b) hormonal induction of cytochrome P450 drug metabolizing enzymes, and (c) hormonal effects on neurotransmission, have all been proposed to underlie the clustering of seizures (Penovich and Helmers, 2008). However, the triggering mechanism of many other types of cyclical seizures, including the seizures caused by MSO, has not been identified. Particularly because MSO is delivered continuously to the hippocampus in male rats, it is rather puzzling that the recurrent seizures occur in clusters. Further studies are required to adequately address this issue.

The behavior and EEG of the seizures in the present model share many similarities with those of human MTLE. A large proportion of the seizures in the MSO-treated rats were characterized initially by immobility (Stage I) that developed into stereotypical head and facial movements, such as eye blinking, head nodding and chewing (Stage II). These events sometimes led to rearing and clonic movements of the forelimbs. These behavioral manifestations are akin to those observed in human MTLE (Engel, 1989). Considerable similarity also exists between the EEG characteristics of seizures observed in the MSO animal model and those of human MTLE. In both instances seizures can begin with high-frequency activity (low-voltage fast activity), which then evolves into lower-frequency, higher-amplitude, more-regular activity. We did not always observe high-frequency discharges at seizure onset in the MSO model, possibly because the recording electrode is placed in the dorsal hippocampus, while the cannula and presumed location of seizure onset are in the ventral hippocampus. High-frequency discharges at seizure onset are often considered a marker for proximity of the electrode to the region of seizure onset.

In agreement with earlier studies, the histopathological changes associated with the present model ranged from virtually no detectable neuronal loss in the hippocampus, via a hippocampal sclerosis-like picture (Gloor, 1991;Sommer, 1880), to extensive neurodegeneration and glial proliferation in some animals (Eid, et al., 2008). We were unable to detect a relationship between the type of neuropathology and the frequency of seizures during either the initial cluster or later clusters (data not shown). However, it is possible that a relationship would be found if more animals were analyzed and if more-sensitive methods to assess the histopathological changes were used. The observation that many animals experienced only minimal neuronal loss in the hippocampus is in agreement with results of human studies. Approximately one-third of all patients surgically treated for temporal lobe epilepsy are characterized by a lack of significant neuronal loss in the resected hippocampus (de Lanerolle, et al., 2003). The remaining two-thirds of patients exhibit hippocampal sclerosis (i.e., glial proliferation with preferential loss of neurons in CA1, CA3 and polymorphic layer of the

dentate hilus) (de Lanerolle, et al., 2003). Notably, the degree of neuronal loss in the hippocampus in this category is highly variable, ranging from extensive neuronal loss to nearly undetectable degeneration by subjective, nonquantitative methods.

What is the mechanism of seizures in the present model? Because MSO inhibits glutamine synthetase, it is possible that the seizures are caused by perturbations in the glutamine-glutamate-GABA metabolism (Ronzio and Meister, 1968). Glutamine synthetase is an integral element of the glutamate-glutamine cycle, which is critically involved in synthesis and degradation of neurotransmitter glutamate (Martinez-Hernandez, et al., 1977). Briefly, glutamate released from neurons during synaptic activity is taken up by astrocytes and converted to glutamine via glutamine synthetase, which in the brain is preferentially present in the cytosol of astrocytes. Glutamine may then be released from the astrocytes, taken up by neurons and converted enzymatically to glutamate (Danbolt, 2001). A deficiency in glutamine synthetase is likely to slow the conversion of glutamate to glutamine and can potentially lead to increased intracellular concentrations of glutamate in astrocytes, with reduced uptake of excitotoxic glutamate from the extracellular space as one of the consequences (Eid, et al., 2004;Laake, et al., 1995;Otis and Jahr, 1998). It is also possible that the glutamine synthetase-deficient astrocytes may release excess intracellular glutamate into the extracellular space, causing hyperexcitability and seizures, as suggested by in vitro and tissue studies (Kimelberg, et al., 1990;Tian, et al., 2005;Volterra and Steinhauser, 2004). A third possibility is that low levels of glutamine synthetase may cause disinhibition, due to impaired vesicular release of GABA (Liang, et al., 2006). After blocking glutamine synthetase by MSO in slice preparations of the hippocampus, Liang and colleagues found a reduction in evoked inhibitory postsynaptic currents in CA1.

MSO has several other effects that may be involved in the triggering of seizures in the present model. MSO inhibits gamma-glutamylcysteine synthetase and causes depletion of the free radical scavenger glutathione (Shaw and Bains, 2002). Deficiency in glutathione has been shown to potentiate seizures and neuronal damage in some animal models (Abe, et al., 2000;Suzer, et al., 2000), whereas in other models a lack of glutathione paradoxically increases the seizure threshold and protects against neuronal damage (Jiang, et al., 2000). However, the tissue levels of glutathione are not changed during the course of the study in our model, and a deficiency in glutathione can therefore not be used to explain the seizures (Eid, et al., 2008). MSO has also been shown to cause accumulation of glycogen in astrocytes, and it has been proposed that this phenomenon is involved in epileptogenesis (Cloix and Hevor, 2009), particularly since high concentrations of brain glycogen are present in the hippocampus in human MTLE (Dalsgaard, et al., 2007). The exact role of brain glycogen in epileptogenesis remains obscure, but studies have suggested that accumulation of glycogen in astrocytes may deprive neurons of energy and consequently result in seizures (Cloix and Hevor, 2009;Hevor, et al., 1986).

In summary, the model of continuous infusion of MSO into the hippocampus in rats reliably and efficiently results in clusters of recurrent, mainly partial seizures that progress over time. The model replicates key features of human MTLE and may prove to be a highly useful tool for mechanistic studies of the development, triggering and clustering of seizures in this disease. A key issue for future studies will be to explore the relationship among the glutamine synthetase deficiency, the concentration of extracellular brain glutamate, and the development of seizures. The working hypothesis is that a deficiency in hippocampal glutamine synthetase leads to high extracellular glutamate concentrations and recurrent seizures. It will also be important to assess the effects of standard antiepileptic drugs on the MSO-induced seizures. The question is whether the MSO-infused animals are resistant to the same type of antiepileptic drugs as patients with medically intractable MTLE.

Abbreviations

AP	anteroposterior
CA1 to CA3	hippocampal subfields cornu ammonis 1 to 3
DV	dorsoventral
EEG	electroencephalogram
GABA	gamma-aminobutyric acid
ML	mediolateral
MSO	methionine sulfoximine
MTLE	mesial temporal lobe epilepsy
PB	phosphate buffer
UV	ultraviolet

Acknowledgments

We thank Ms. Ilona Kovacs for excellent technical assistance, Ms. Anne Sommer for editorial advice and Dr. Robert Duckrow for helpful discussions. This work was supported by a grant from National Institutes of Health (NS054801 to T.E.)

References

Abe K, Nakanishi K, Saito H. The possible role of endogenous glutathione as an anticonvulsant in mice. Brain Res 2000;854:235–238. [PubMed: 10784128]

Amaral, DG.; Insausti, R. Hippocampal formation. In: Paxinos, G., editor. The human nervous system. San Diego: Academic Press; 1990. p. 711-756.

Avoli, M.; Gloor, P. Pathophysiology of focal and generalized convulsive seizures versus that of generalized non-convulsive seizures. In: Wolf, P., editor. Epileptic Seizures and Syndromes. Montrouge, France: John Libbey Eurotext Ltd; 1994. p. 547-561.

Balish M, Albert PS, Theodore WH. Seizure frequency in intractable partial epilepsy: a statistical analysis. Epilepsia 1991;32:642–649. [PubMed: 1915170]

Bauer J, Burr W. Course of chronic focal epilepsy resistant to anticonvulsant treatment. Seizure 2001;10:239–246. [PubMed: 11466018]

Ben-Ari Y. Limbic seizure and brain damage produced by kainic acid: mechanisms and relevance to human temporal lobe epilepsy. Neuroscience 1985;14:375–403. [PubMed: 2859548]

Ben-Ari Y. Epilepsies and neuronal plasticity: for better or for worse? Dialogues Clin Neurosci 2008;10:17–27. [PubMed: 18472481]

Bernard-Helary K, Lapouble E, Ardourel M, Hevor T, Cloix JF. Correlation between brain glycogen and convulsive state in mice submitted to methionine sulfoximine. Life Sci 2000;67:1773–1781. [PubMed: 11021361]

Bertram EH, Williamson JM, Cornett JF, Chen ZF. Design and construction of a long-term continuous video-EEG monitoring unit for simultaneous recording of multiple small animals. Brain Res. Brain Res. Protoc 1997;1997:85–97.

Blume WT. The progression of epilepsy. Epilepsia 2006;47 Suppl 1:71–78. [PubMed: 17044831]

Cavus I, Kasoff WS, Cassaday MP, Jacob R, Gueorguieva R, Sherwin RS, Krystal JH, Spencer DD, Abi-Saab WM. Extracellular metabolites in the cortex and hippocampus of epileptic patients. Ann Neurol 2005;57:226–235. [PubMed: 15668975]

Cendes F, Andermann F, Dubeau F. Early childhood prolonged febrile convulsions, atrophy and sclerosis of mesial structures, and temporal lobe epilepsy; A MRI volumetric study. Neurology 1993;43:1083–1087. [PubMed: 8170546]

Cloix JF, Hevor T. Epilepsy, regulation of brain energy metabolism and neurotransmission. Curr Med Chem 2009;16:841–853. [PubMed: 19275597]

Dalsgaard MK, Madsen FF, Secher NH, Laursen H, Quistorff B. High glycogen levels in the hippocampus of patients with epilepsy. J Cereb Blood Flow Metab 2007;27:1137–1141. [PubMed: 17133225]

Danbolt NC. Glutamate uptake. Prog. Neurobiol 2001;65:1–105. [PubMed: 11369436]

de Lanerolle NC, Kim JH, Williamson A, Spencer SS, Zaveri HP, Eid T, Spencer DD. A retrospective analysis of hippocampal pathology in human temporal lobe epilepsy: Evidence for distinctive patient subcategories. Epilepsia 2003;44:677–687. [PubMed: 12752467]

Dube C, Chen K, Eghbal-Ahmadi M, Brunson K, Soltesz I, Baram TZ. Prolonged febrile seizures in the immature rat model enhance hippocampal excitability long term. Ann Neurol 2000;47:336–344. [PubMed: 10716253]

Dudek, FE.; Clark, S.; Williamns, PA.; Grabenstatter, HL. Kainate-induced status epilepticus: a chronic model of acquired epilepsy. In: Pitkanen, A.; Schwartzkroin, PA.; Solomon, LM., editors. Models of Seizures and Epilepsy. Burlington: Elsevier Academic Press; 2006. p. 415-432.

During MJ, Spencer DD. Extracellular hippocampal glutamate and spontaneous seizure in the conscious human brain. Lancet 1993;341:1607–1610. [PubMed: 8099987]

Eid T, Ghosh A, Wang Y, Beckstrom H, Zaveri HP, Lee TS, Lai JC, Malthankar-Phatak GH, de Lanerolle NC. Recurrent seizures and brain pathology after inhibition of glutamine synthetase in the hippocampus in rats. Brain 2008;131:2061–2070. [PubMed: 18669513]

Eid T, Thomas MJ, Spencer DD, Runden-Pran E, Lai JC, Malthankar GV, Kim JH, Danbolt NC, Ottersen OP, de Lanerolle NC. Loss of glutamine synthetase in the human epileptogenic hippocampus: possible mechanism for raised extracellular glutamate in mesial temporal lobe epilepsy. Lancet 2004;363:28–37. [PubMed: 14723991]

Engel, J, Jr. Seizures and Epilepsy. Philadelphia: F. A. Davis Company; 1989.

Folbergrova J, Passonneau JV, Lowry OH, Schulz DW. Glycogen, ammonia and related metabolities in the brain during seizures evoked by methionine sulphoximine. J Neurochem 1969;16:191–203. [PubMed: 5795934]

French JA, Williamson PD, Thadani VM, Darcey TM, Mattson RH, Spencer SS, Spencer DD. Characteristics of medial temporal lobe epilepsy: I. Results of history and physical examination. Ann Neurol 1993;34:774–780. [PubMed: 8250525]

Gloor, P. Mesial temporal sclerosis: Historical background and an overview from a modern perspective. In: Luders, H., editor. Epilepsy Surgery. New York: Raven Press; 1991. p. 6889-6703.

Goffin K, Nissinen J, Van Laere K, Pitkanen A. Cyclicity of spontaneous recurrent seizures in pilocarpine model of temporal lobe epilepsy in rat. Exp Neurol 2007;205:501–505. [PubMed: 17442304]

Herzog AG, Harden CL, Liporace J, Pennell P, Schomer DL, Sperling M, Fowler K, Nikolov B, Shuman S, Newman M. Frequency of catamenial seizure exacerbation in women with localization-related epilepsy. Ann Neurol 2004;56:431–434. [PubMed: 15349872]

Hevor TK, Delorme P, Beauvillian JC. Glycogen synthesis and immunocytochemical study of fructose-1,6-Biphosphatase in methionine sulfoximine epileptogenic rodent brain. 1986;6:292–297.

Jefferys, JGR.; Walker, MC. Tetanus toxin model of focal epilepsy. In: Pitkanen, A.; Schwartzkroin, PA.; Moshe, SL., editors. Models of Seizures and Epilepsy. Amsterdam: Elsevier Academic Press; 2006. p. 407-414.

Jiang D, Akopian G, Ho YS, Walsh JP, Andersen JK. Chronic brain oxidation in a glutathione peroxidase knockout mouse model results in increased resistance to induced epileptic seizures. Exp Neurol 2000;164:257–268. [PubMed: 10915565]

Joels M. Stress, the hippocampus, and epilepsy. Epilepsia 2009;50:586–597. [PubMed: 19054412]

Kimelberg HK, Goderie SK, Higman S, Pang S, Waniewski RA. Swelling-induced release of glutamate, aspartate, and taurine from astrocyte cultures. J. Neurosci 1990;10:1583–1591. [PubMed: 1970603]

Laake JH, Slyngstad TA, Haug FM, Ottersen OP. Glutamine from glial cells is essential for the maintenance of the nerve terminal pool of glutamate: immunogold evidence from hippocampal slice cultures. J Neurochem 1995;65:871–881. [PubMed: 7616248]

Liang SL, Carlson GC, Coulter DA. Dynamic regulation of synaptic GABA release by the glutamate-glutamine cycle in hippocampal area CA1. J Neurosci 2006;26:8537–8548. [PubMed: 16914680]

Lorente de Nó R. Studies on the structure of the cerebral cortex. II. Continuation of the study of the ammonic system. J. Psychol. Neurol. (Leipzig) 1934;46:113–177.

Martinez-Hernandez A, Bell KP, Norenberg MD. Glutamine synthetase: glial localization in brain. Science 1977;195:1356–1358. [PubMed: 14400]

McIntyre DC, Kelly ME, Dufresne C. FAST and SLOW amygdala kindling rat strains: comparison of amygdala, hippocampal, piriform and perirhinal cortex kindling. Epilepsy Res 1999;35:197–209. [PubMed: 10413315]

Otis TS, Jahr CE. Anion currents and predicted glutamate flux through a neuronal glutamate transporter. J Neurosci 1998;18:7099–7110. [PubMed: 9736633]

Penovich PE, Helmers S. Catamenial epilepsy. Int Rev Neurobiol 2008;83:79–90. [PubMed: 18929076]

Petroff OA, Errante LD, Rothman DL, Kim JH, Spencer DD. Glutamate-glutamine cycling in the epileptic human hippocampus. Epilepsia 2002;43:703–710. [PubMed: 12102672]

Racine RJ, Burnham WM, Gartner JG, Levitan D. Rates of motor seizure development in rats subjected to electrical brain stimulation: strain and inter-stimulation interval effects. Electroencephalogr Clin Neurophysiol 1973;35:553–556. [PubMed: 4126463]

Ronzio RA, Meister A. Phosphorylation of methionine sulfoximine by glutamine synthetase. Proc Natl Acad Sci U S A 1968;59:164–170. [PubMed: 5242120]

Shaw CA, Bains JS. Synergistic versus antagonistic actions of glutamate and glutathione: the role of excitotoxicity and oxidative stress in neuronal disease. Cell Mol Biol (Noisy-le-grand) 2002;48:127–136. [PubMed: 11990449]

Sommer W. Erkrankung des Ammonshorns als aetiologisches Moment der Epilepsie. Arch. Psychiatr. Nervenkr 1880;10:631–675.

Steffens M, Huppertz HJ, Zentner J, Chauzit E, Feuerstein TJ. Unchanged glutamine synthetase activity and increased NMDA receptor density in epileptic human neocortex: implications for the pathophysiology of epilepsy. Neurochem Int 2005;47:379–384. [PubMed: 16095760]

Subbalakshmi GY, Murthy CR. Effects of methionine sulfoximine on cerebral ATPase. Biochem Pharmacol 1981;30:2127–2130. [PubMed: 6117282]

Suzer T, Coskun E, Demir S, Tahta K. Lipid peroxidation and glutathione levels after cortical injection of ferric chloride in rats: effect of trimetazidine and deferoxamine. Res Exp Med (Berl) 2000;199:223–229. [PubMed: 10743680]

Szegedy L. Enzyme histochemical studies in the rat hippocampus, cerebellar cortex and brainstem motor nuclei during methionine sulphoximine convulsions. Cell Mol Biol 1978;23:43–53.

Tian GF, Azmi H, Takano T, Xu Q, Peng W, Lin J, Oberheim N, Lou N, Wang X, Zielke HR, Kang J, Nedergaard M. An astrocytic basis of epilepsy. Nat Med 2005;11:973–981. [PubMed: 16116433]

Turski WA, Cavalheiro EA, Schwarcz M, Czuczwar SZ, Kleinrok Z, Turski L. Limbic seizures produced by pilocarpine in rats: behavioral, electroencephalographic and neuropathological study. Behav. Brain Res 1983;9:315–335. [PubMed: 6639740]

van der Hel WS, Notenboom RG, Bos IW, van Rijen PC, van Veelen CW, de Graan PN. Reduced glutamine synthetase in hippocampal areas with neuron loss in temporal lobe epilepsy. Neurology 2005;64:326–333. [PubMed: 15668432]

Vezzani A, Granata T. Brain inflammation in epilepsy: experimental and clinical evidence. Epilepsia 2005;46:1724–1743. [PubMed: 16302852]

Volterra A, Steinhauser C. Glial modulation of synaptic transmission in the hippocampus. Glia 2004;47:249–257. [PubMed: 15252814]

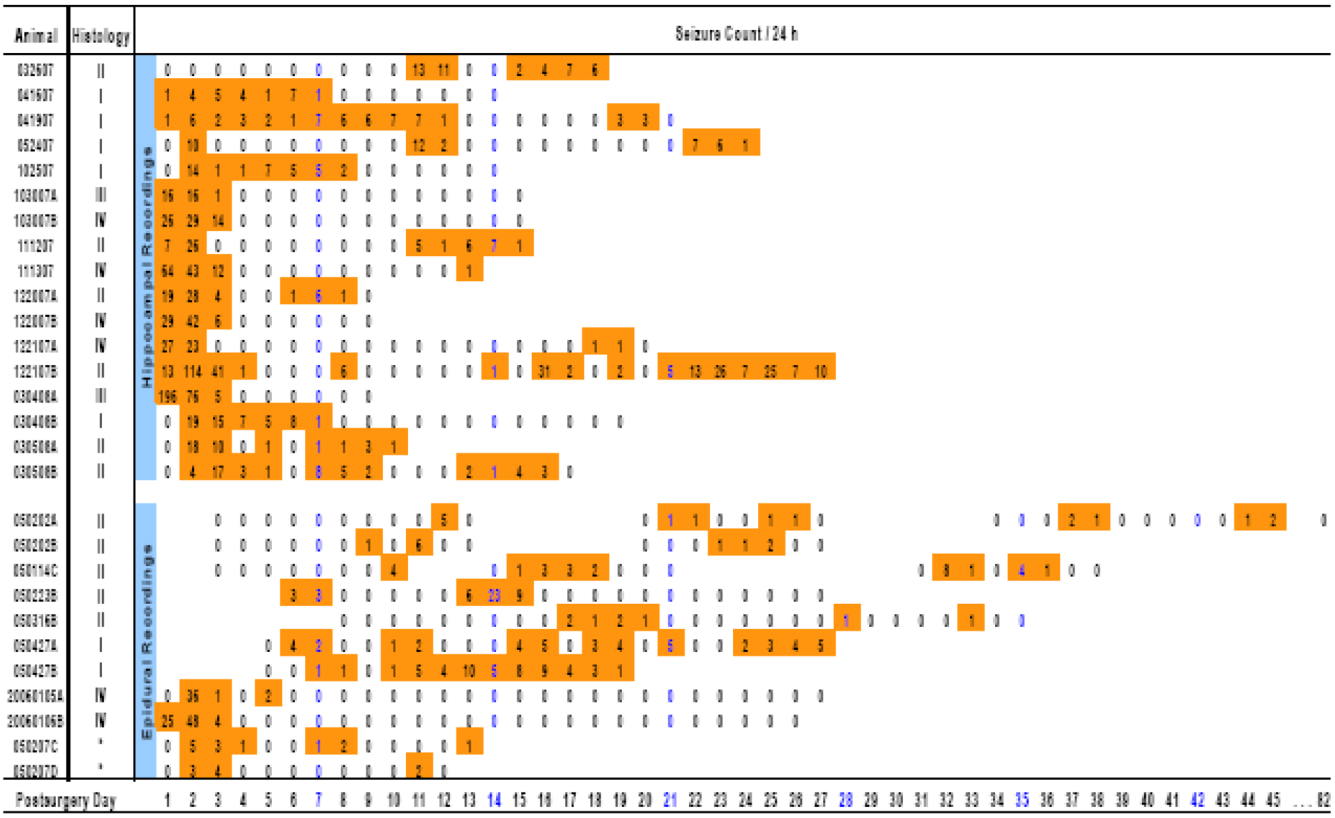

Figure 1. Overview of the temporal distribution of seizures and histopathological changes in MSO-treated animals

Seventeen animals were recorded by continuous hippocampal depth electrode video-EEG (top group) and 11 animals were recorded by intermittent epidural screw electrode video-EEG (bottom group). Seizure counts are given and shown in color. Note the presence of an initial cluster of very frequent seizures in many animals. Subsequent clusters of seizures occurred throughout the monitoring period, which extended as far as 82 days for one of the animals. The histopathological classification into Grades I to IV is described in detail in the legend to Fig. 6. No tissue was available for histology from animals 050207C and 050207D (indicated by asterisks).

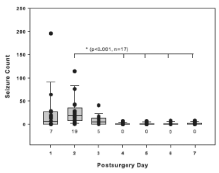

Figure 2. Daily frequency of seizures during the first 7 days of MSO infusion

The daily counts of seizures in the 17 MSO-treated, depth electrode-recorded animals are depicted by boxplots and vertical point plots (which are superimposed on the boxplots). The seizure frequency during postsurgical day 2 was significantly higher than that during postsurgical days 4 to 7 ($p < 0.001$, Kruskal-Wallis analysis followed by Dunn's test, $n = 17$). Boxes contain the 25th to 75th percentiles of the data and whiskers the 10th to 90th percentiles. The median is indicated by the horizontal line across the box and the number below each plot. The individual data points are also indicated by black dots.

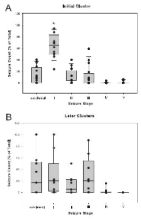

Figure 3. Distribution of seizure stages during the initial and later seizure clusters

The number (fractional distribution) of seizures within each seizure stage was determined by randomized sampling for the initial cluster (A) and all of the later clusters combined (B) in the depth-electrode implanted, MSO-treated animals. The fractional distribution of seizures at different stages is indicated by boxplots and vertical point plots (which are superimposed on the boxplots). Each data point (black dot) represents the average number of seizures from one animal. The median number of Stage I seizures is significantly higher than the median number of seizures of any other stage during the initial cluster ($p < 0.001$, Kruskal-Wallis analysis followed by Dunn's test, $n = 16$). See the legend to Fig. 2 for an explanation of the plots.

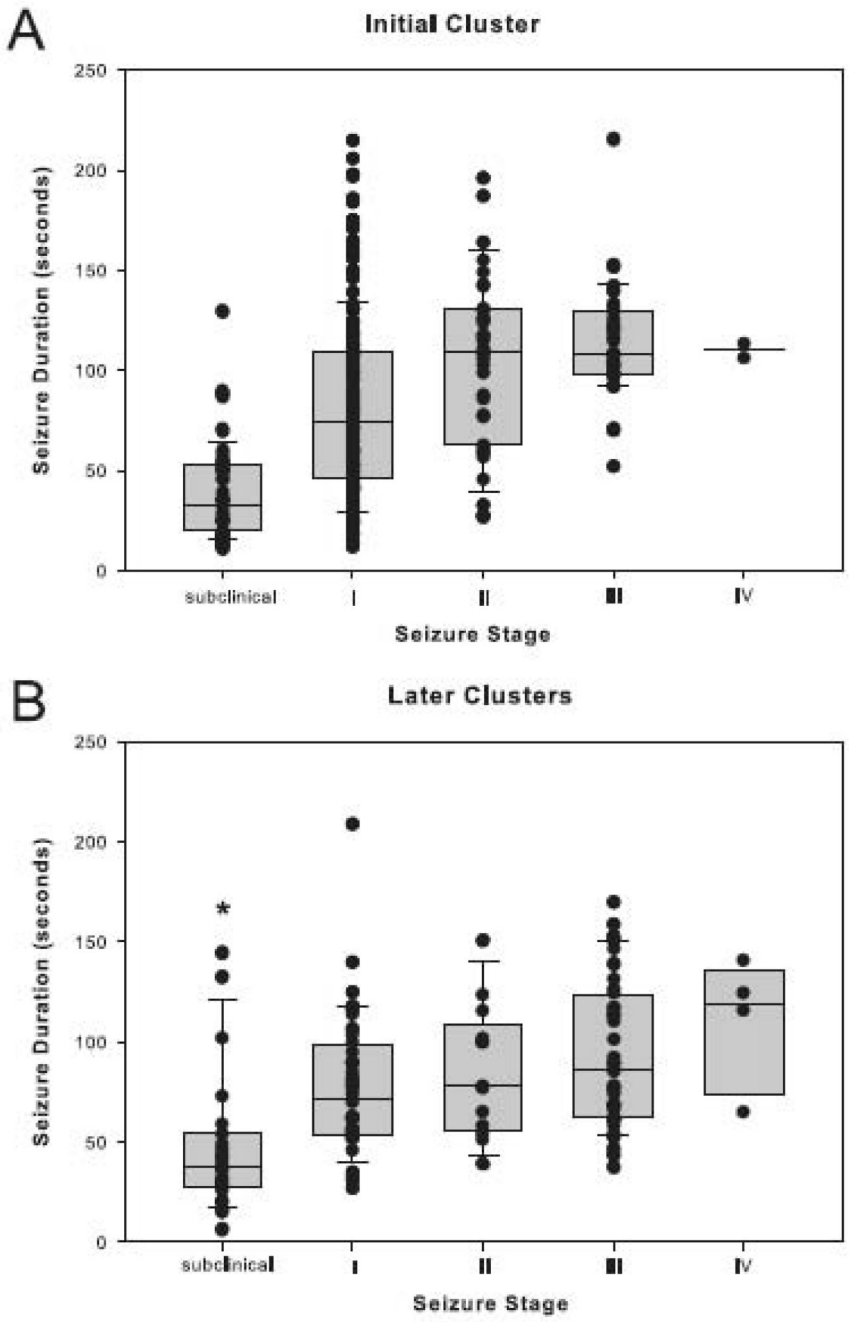

Figure 4. Duration of each seizure stage during the initial and later seizure clusters

The durations (in seconds) of seizures within each seizure stage were determined by randomized sampling for the initial cluster (A) and all of the later clusters combined (B) in the depth-electrode implanted, MSO-treated animals. The data are indicated by boxplots and vertical point plots (which are superimposed on the boxplots) for the initial cluster (A) and all of the later clusters combined (B), in the depth-electrode implanted, MSO-treated animals. The median duration of subclinical seizures is significantly shorter than the median duration of seizures of the other stages in the later clusters (difference indicated by asterisk; $p < 0.001$, Kruskal-Wallis analysis followed by Dunn's test, $n = 16$). Moreover, the median duration of Stage III seizures is shorter in the later clusters than the initial cluster ($p < 0.01$, Mann-Whitney

Rank Sum test, difference not indicated by asterisk). Due to the very small number of Stage V seizures, no such seizures were sampled in the analysis of seizure duration; hence, the absence of data from Stage V. See the legend to Fig. 2 for an explanation of the plots.

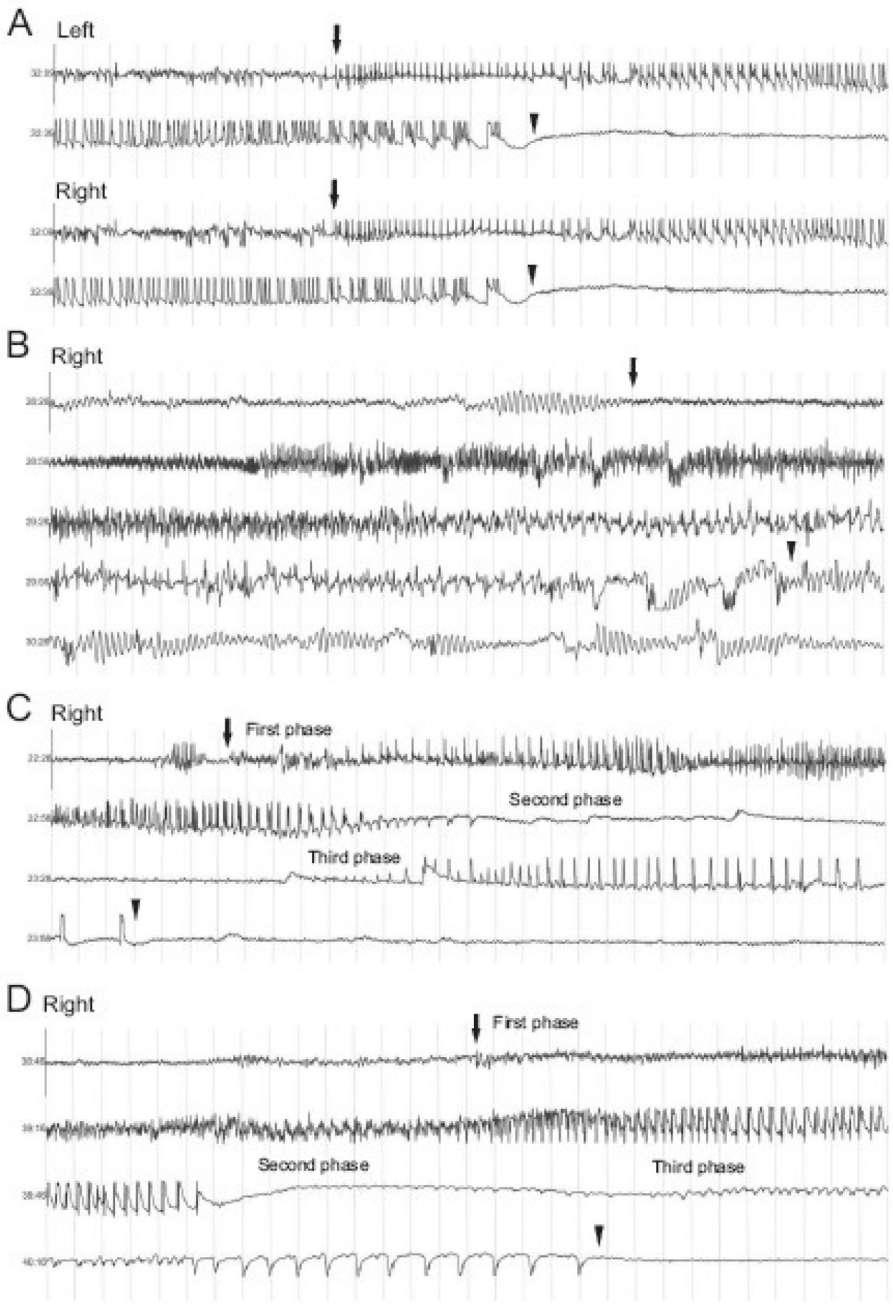

Figure 5. Representative traces of intrahippocampal depth electrode EEGs from MSO-treated rats

Continuous EEG traces recorded from a depth electrode in either the left or right hippocampus are shown in A–C and from an epidural screw electrode are shown in D. Thirty seconds of EEG is displayed in each trace. The light gray vertical lines demarcate 1-second time intervals, and the Y axis in each figure corresponds to 5 mV (±2.5 mV). The seizures in A – D were recorded from different animals. Seizure onset and offset are marked with arrows with the first arrow marking seizure onset and the second arrow marking seizure offset. Two main types of ictal EEG patterns were observed: Type I Seizures (A and B) and Type II Seizures (C and D). Both types of seizures could begin with high-frequency EEG activity, though this was not always observed. Then the EEG frequency decreased, while the amplitude slowly built up and

the activity became more regular. A seizure with lack of high-frequency onset signal is seen in A. The high-amplitude, low-frequency EEG discharges usually lasted 30 to 60 seconds, though longer-duration Type I Seizures could also be observed (B); then the seizure stopped and the EEG became quiet. Very low-amplitude rhythmic delta activity, which continued for several seconds, was occasionally present after the seizure (A). Higher-amplitude postictal delta activity was occasionally seen as well (B). The Type II Seizure (C and D) was characterized by a third phase of ictal activity that followed a quiet period, which typically lasted 10 to 30 seconds. This third phase of the seizure was characterized by high-amplitude spike discharges that lasted 5 to 20 seconds.

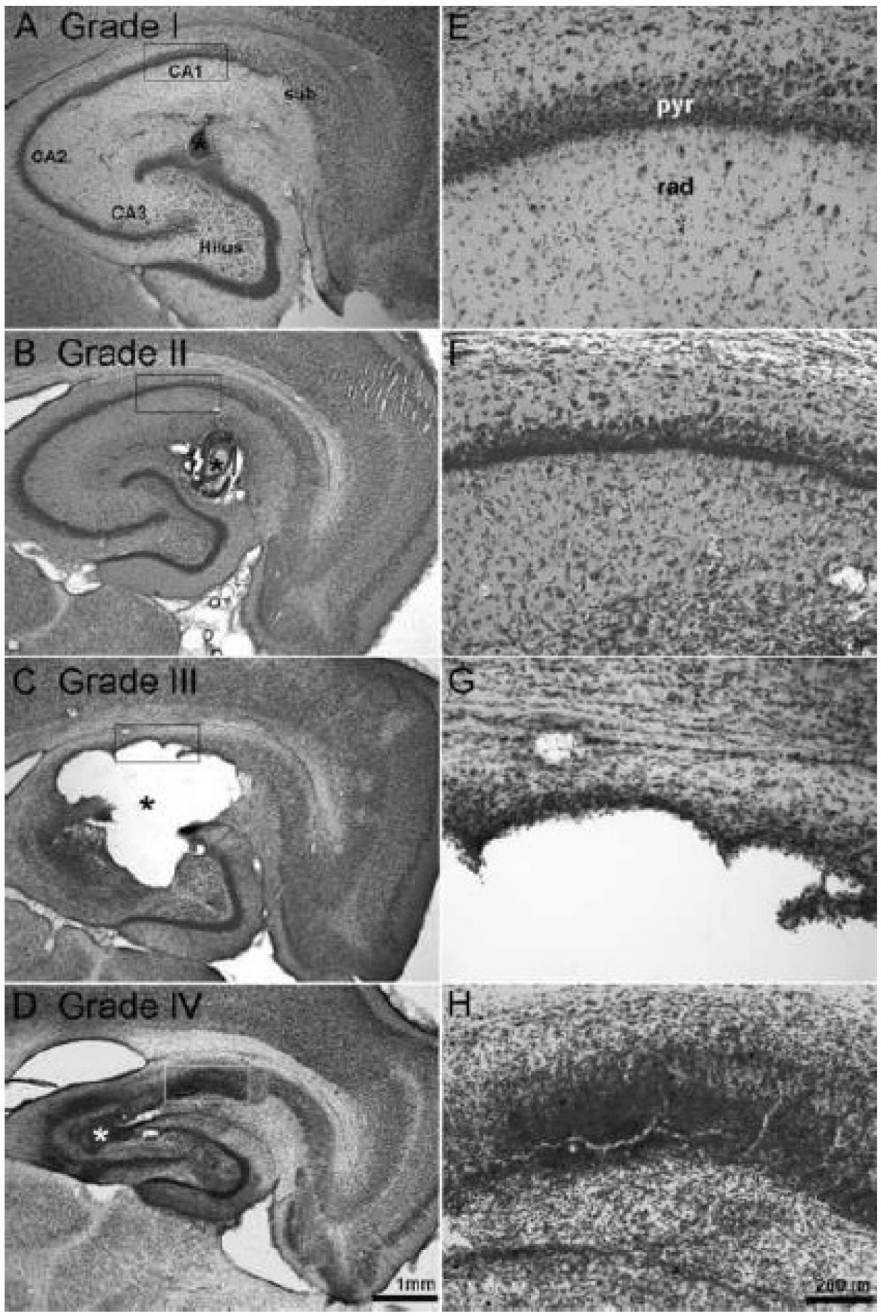

Figure 6. Histopathological changes of the hippocampus after chronic infusion with MSO

(A to D) Nissl-stained horizontal sections of the hippocampus from 4 representative rats treated with continuous infusion of 0.625 μg of MSO per h and continuously recorded by video-intracranial EEG. (E to H) High-power fields of CA1, as indicated by the rectangular boxes in A to D, respectively. Four grades of histopathological changes were apparent: Grade I (A, E), minimal neuronal loss (diameter, <100 μm) and gliosis around the infusion cannula track, no patterned involvement of other hippocampal subfields; Grade II (B, F), more extensive neuronal loss (diameter, >100 μm) around the infusion cannula track, necrosis is not present; Grade III (C, G), large (diameter, >100 μm) necrotic lesions involving and usually extending beyond the hippocampus; Grade IV (D, H), hippocampal sclerosis-like changes with atrophy

of the hippocampus and loss of neurons in CA1 to CA3 and the dentate hilus, marked glial proliferation. Abbreviations: sub, subiculum; CA1 to CA3, hippocampal subfields cornu ammonis 1 to 3; pyr, pyramidal layer; rad, stratum radiatum. Scale bar: 1 mm in A to D; 200 μm in E to H. Asterisks in A to D indicate the position of the MSO infusion cannula.